International Journal of Advance Research in Science and Engineering
Vol. No.6, Issue No. 07, July 2017
www.ijarse.com
IJARSE
ISSN (O) 2319 - 8354
ISSN (P) 2319 - 8346

Photodegradation of Congo red azo dye, a Carcinogenic Textile dye by using synthesized Nickel Calciate Nanoparticles

Santhosh A. M.[1], Yogendra K.[2], Mahadevan K. M.[3], Madhusudhana N.[4]

[1,4]Department of P.G studies and Research in Environmental Science, Kuvempu University, Jnana Sahyadri, Shankaraghatta, Shivamogga, Karnataka (India)

[3]Department of Chemistry, Kadur P.G Center, Kuvempu University, Kadur, Karnataka (India)

[2]Assistant Professor, Department of P.G Studies and Research in Environmental Science, Kuvempu University, Jnana Sahyadri, Shankaraghatta, Shimoga, Karnataka (India)

ABSTRACT

The photodegradation of Congo Red (CR) by using nickel calciate nanoparticles ($NiCaO_2$) was investigated. The Nickel calciate nanoparticles ($NiCaO_2$) were prepared by solution combustion method using urea and acetamide as fuels and they were characterized by Scanning Electron Micrograph (SEM), X-Ray Diffraction (XRD), Energy Dispersive X-ray (EDX), Brunauer Emmett-Teller surface area determination and band gap was determined by using UV-absorption spectroscopy. Point zero charge determined by pH drift method. All experiments were carried out under natural sun light. Examined the percentage of degradation of these nanoparticles on Congo Red by varying the dye concentration, pH and catalyst loading. The percentage of degradation was highly efficient in 20ppm dye concentration with pH 4 and constant catalyst concentration 0.4g/100ml for both nanoparticles. This proves that, synthesized nickel calciate nanoparticles are efficient in removing the Congo Red from the waste water.

Keyword: Congo red, Nickel Calciate, Nanoparticles, Photodegradation

I. INTRODUCTION

Azo dyes are majorly used in the textile industries and also used in paper making, pharmacy, textile, cosmetics and food processing [3]. These azo dyes are known to be largely non-biodegradable, because which characterized by one or more azo groups (-N=N-) and the release of these azo compounds into water streams is undesirable, it can cause toxic or mutagenic to the living organisms by not only the colour, due to their breakdown products of many azo dyes [4,5]. Under aerobic conditions and their stability is proportional to the structural complexity of their molecular structures [6]. Azo dyes resistant to aerobic degradation but under anaerobic conditions they can be reduced to potentially carcinogenic aromatic amines [7].

Congo red widely used in textile, printing and dyeing, paper, rubber and plastic industries and banned in, many countries because of health concerns. Synthetic dyes, such as CR, are difficult to biodegrade due to their stable compounds and complex aromatic structures and affects carcinogen and mutagen [8-12]. Various physical and chemical treatment methods are employed for the removal of azo dyes from the aqueous solution such as, chemical precipitation, activated carbon, ultra-filtration, adsorption, coagulation, membrane filtration, biological

IJARSE
ISSN (O) 2319 - 8354
ISSN (P) 2319 - 8346

degradation, and oxidation via ozonation. But, these methods are costly, ineffective non-destructive, simply they can transfer the pollutant from one phase to another phase and produce secondary pollutants waste products that need further disposal [4,7,13,14]. In recent years an alternative to conventional methods, *i.e.* "Advanced Oxidation Processes" (AOPs), based on the generation of reactive species (hydroxyl radicals), mainly hydroxyl radicals by using solar, chemical or other forms of energy, that strongly oxidizing radical allows the destruction ofbroad range of organic pollutants [13,15,16].

Other researcher has investigated the degradation of CR in presence of different catalysts [8, 17-23]. In this study newly synthesized nickel calciate nanoparticles were applied to degrade the CR azo dye by varying the different parameters such as, initial dye concentration, pH, catalyst loading and in different conditions with respect to UV light and dark conditions.

II. MATERIALS AND METHODS

The commercially available water soluble dyes Congo Red (λ_{max}496nm) were obtained from Sisco Research Laboratory Pvt. Ltd. Maharashtra (Figure 1). The chemicals Nickel Nitrate ($Ni(NO_3)_2.6H_2O$) (99% A. R.), obtained from Sisco Research Laboratory Pvt. Ltd. Maharastra Calcium Nitrate ($Ca(NO_3)_2.4H_2O$) (99%, A. R.), Urea (NH_2CONH_2) (99.5%), Acetamide (CH_3CONH_2) (99%, A.R.), were obtained from Hi-Media Chemicals, Mumbai. The visible spectrophotometer (Elico, SL 177) has been used for recording absorbance at λ_{max}. Later the absorbance was recorded in visible spectrophotometer (Elico, SL 177).

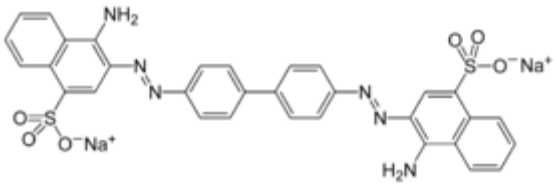

Fig 1: Chemical structure of CR

2.1 Synthesis and Characterization of Nanoparticles

The synthesis of nickel claciate nanoparticles were prepared by solution combustion method by using urea and acetamide as a fuel. The ratios were taken according to stochiometric equation and reaction as follows. The solution taken in crucible was inserted in preheated 600°C muffle furnace and the synthesized nanoparticles was crushed in a mortar to make it amorphous and used for further characterization and application to photocatalytic degradation study of CR dye

$3\ Ni\ (NO_3)_2+3Ca\ (NO_3)_2+10NH_2CONH_2 \rightarrow 3NiCaO_2+10CO_2+20H_2O+16N_2$ (Eq. 1)

$11\ Ni\ (NO_3)_2+11Ca\ (NO_3)_2+20CH_3CONH_2 \rightarrow 11NiCaO_2+50CO_2+40H_2O+32N_2$ (Eq. 2)

Characterization of nanoparticles by Powder X-ray diffraction (XRD) was performed by powder X-ray diffraction (Rigaku diffractrometer) using Cu-Kα radiation (1.5406 Å) in a θ-2θ configuration. Scanning electron microscope (SEM) image was taken with a JEOL (JSM-840A). The UV-visible spectra of the photocatalysts were carried out using a UV-visible spectrophotometer in the λ range from200 to 1200 nm. The confirmatory presence of elements was carried out using Energy Dispersive X-ray (EDX) spectrometer. Specific surface areas (SSA) of all photocatalysts were measured at 77 K by Brunauer–Emmett–Teller (BET) nitrogen adsorption–desorption (NOVA-1000 version 3.70 Instrument).

IJARSE
ISSN (O) 2319 - 8354
ISSN (P) 2319 - 8346

2.2 Point of Zero Charge

Point of zero charge (pzc) or isoelectric point is the pH of the solution at which the total charge on the surface of the nanoparticles becomes zero (neutral). The pzc of $NiCaO_2$ were measured by pH drift method, 50ml of Nacl 0.01M was taken in six separate beaker sand bubbled it with Nitrogen gas to expel the dissolved CO_2 for few minutes at room temperature till it get a stable pH reading. The pH of the solution in each beaker was adjusted between 2 to 12 by adding 0.1N Hcl and 0.1N NaOH after which 50mg of $NiCaO_2$ nanoparticles were added. This system was kept at room temperature until concurrent pH measured; this was kept for 92hrs for the stabilization of pH. The graph was plot against final pH v/s initial pH, the point which this curve crosses the initial pH=final pH straight line is the point of zero charge.

2.3 Experiment Procedure

Photocatalytic experiments were conducted under direct sunlight. The CR solution was prepared by dissolving 0.02 g of azo dye with 1000mL double distilled water using a 1000ml volumetric flask and degradation in the presence of Nickel Calciate nanoparticles at different catalyst dosages pH levels and initial dye concentration. Initially, 100ml of 20ppm of dye samples were tested with different catalyst dosage (from 0. 1g to 1g), by varying pH (from 2pH to 11pH), dye concentration (20ppm to 50ppm) and different conditions with respect to U.V and dark. Except U.V and dark conditions all experiments carried out in the presence of direct sunlight. The whole experimental set-up was placed under sunlight between 11 a.m. and 2 p.m. and the average intensity of sunlight during this period is 834×100 lux unit using lux meter. After the photocatalytic degradation, the extent of degradation was estimated by recording absorbance of the dye solution using spectrophotometer (Elico, SL 177) in order to get the optimum catalyst dose.

The percentage was calculated by equation,

$$D = (C_0 - C_t / C_0 \times 100) \qquad \text{(Eq. 3)}$$

Where, $\mathbf{C_0}$ is the initial absorbance of the dye solution $\mathbf{C_t}$ is absorbance at time interval 't' *i.e.,* after 120 minutes.

III. RESULT AND DISCUSSION

3.1 Characterization of the Nanoparticles

The structural morphology of the nanoparticles looks like foamy in nature [24] (Fig 2a and 2b). In Fig 3 shows the powdered sample of newly synthesized $NiCaO_2$-I and $NiCaO_2$-II nanoparticles were examined by XRD studies and the average crystallite size of $NiCaO_2$-I and $NiCaO_2$-II was found to be 14nm and 19nm respectively. The pattern obtained from the XRD analysis of the prepared $NiCaO_2$ nanoparticles is presented in Fig 3a and 3b and calculated average size of nanoparticles by using Debye Scherrer's formula equation.

$$D = (K \lambda / (\beta \cos\theta)) \qquad \text{(Eq.4)}$$

Fig 4 shows that, the band gap energy of the $NiCaO_2$ nanoparticles was calculated using the following simple conversion equation. The band gap equation is calculated using the Planck's equation as follows.

$$E = h C / \lambda \qquad \text{(Eq. 5)}$$

The band gap energy of nanoparticles was found to be 3.3eV for both $NiCaO_2$ I and $NiCaO_2$ II. The UV-absorbance spectra of synthesized $NiCaO_2$ are presented in Figure 4a and 4b. Figure 5 confirms the presence of Nickel, Calcium, Carbon and Oxygen in Nickel Calciate Nanoparticles. The vertical axis displays the number of

IJARSE
ISSN (O) 2319 - 8354
ISSN (P) 2319 - 8346

x-ray counts although the horizontal axis displays energy in KeV (Fig. 5a and 5b). The weight and atomic percentage of Carbon, Oxygen, Calcium, and Nickel was found to be 7.79, 51.80, 25.74, 14.67 and 13.57, 67.76, 13.44, 5.23 for $NiCaO_2$-I and $NiCaO_2$-II found to be 20.57, 46.88, 17.85, 14.69 and 32.08, 54.88, 8.344.69 these corresponds, the spectrum without impurities peaks [25].

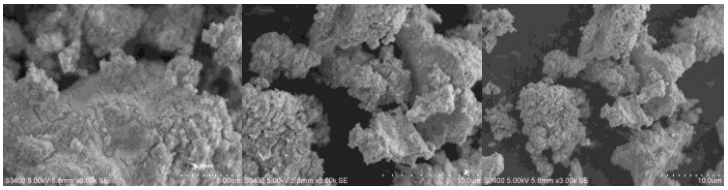

(a)

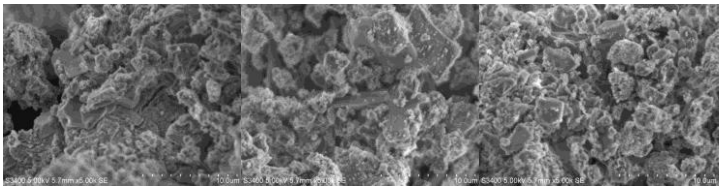

(b)

Fig 2: Scanning Electron Micrographs of synthesized (a) $NiCaO_2$ – I (b) $NiCaO_2$ – II Nanoparticles

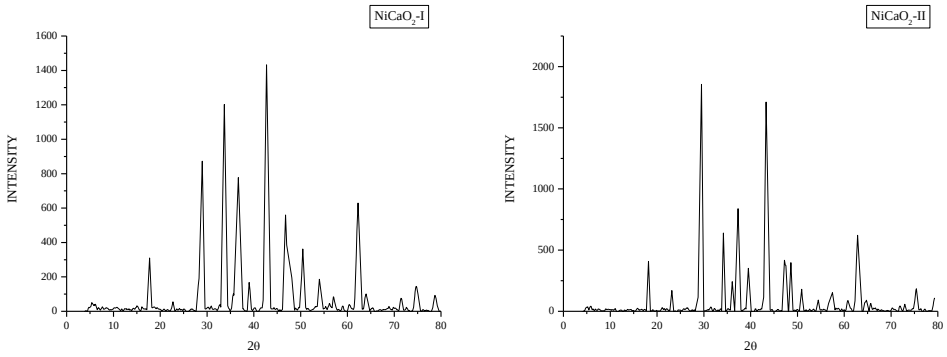

(a) (b)

Fig 3: XRD of the synthesized Nanoparticles (a) $NiCaO_2$-I (b) $NiCaO_2$ -II

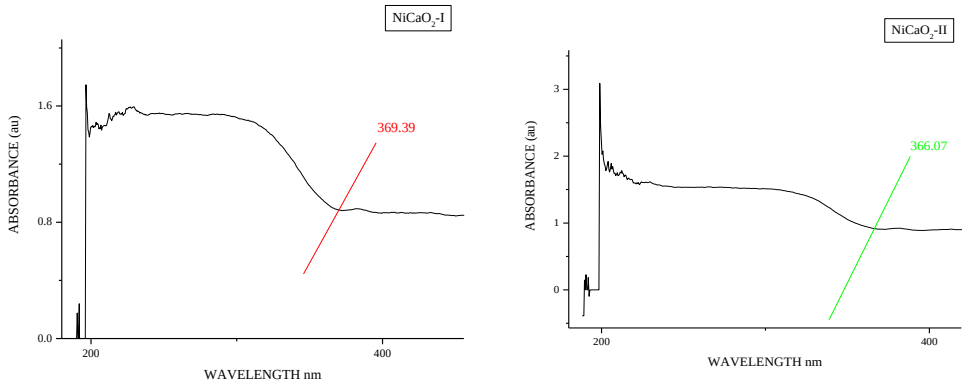

(a) (b)

Fig 4: UV-absorption spectra of synthesized Nanoparticles (a) $NiCaO_2$ – I (b) $NiCaO_2$ – II

International Journal of Advance Research in Science and Engineering
Vol. No.6, Issue No. 07, July 2017
www.ijarse.com
IJARSE
ISSN (O) 2319 - 8354
ISSN (P) 2319 - 8346

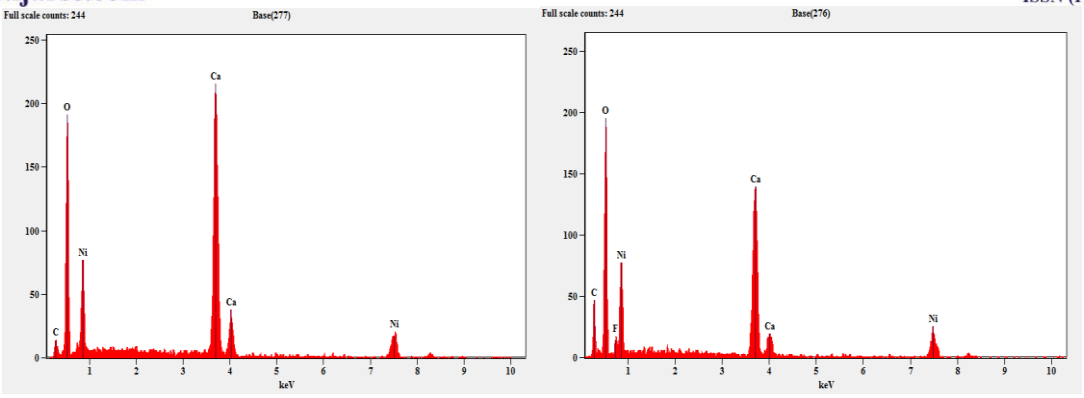

(a) (b)

Fig 5: Energy Dispersive X-ray of synthesized Nanoparticles (a) $NiCaO_2$– I (b) $NiCaO_2$ – II

3.2 Bet Surface Area Analysis

The catalytic activity of the nanoparticles is closely related to their porous structure facilitating the contact with the pollutant which favours positively to the photocatalytic activity. Using the BET surface area analysis, the specific surface area, pore volume and average pore diameter for $NiCaO_2$ nanoparticles are depicted in table 1. This value is analogues to the other nanoparticles [26-29]. The obtained surface area for $NiCaO_2$ nanoparticles is suitable to carry out the photocatalysis as the photoelectric conversion efficiency is directly proportional to the surface area available [30].

Table 1: Surface properties of the nanoparticles

Catalyst	Surface area	Pore volume	Average pore diameter
$NiCaO_2$ (urea)	2.4416 m^2/g	0.01013 cc/g	165.87Å
$NiCaO_2$ (acetamide)	2.3778 m^2/g	0.00265 cc/g	44.578Å

3.3 Nature of Point of Zero Charge

In order to understand the behaviour of adsorption or photocatalysts with respect to pH it is important to determine the isoelectric point or point zero charge of the nanoparticles. For the determination of pzc of $NiCaO_2$ nanoparticles, graph of initial pH against final pH was plotted and the values of $pH_{(pzc)}$ were found to be 11.5 and 11.7 (Fig 6). Below this $pH_{(pzc)}$ the surface is positively charged and above this surface negatively charged. The pH of CR is below the $pH_{(pzc)}$, which favours the degradation of anionic CR and thus the suitable for photocatalysis [30]

IJARSE
ISSN (O) 2319 - 8354
ISSN (P) 2319 - 8346

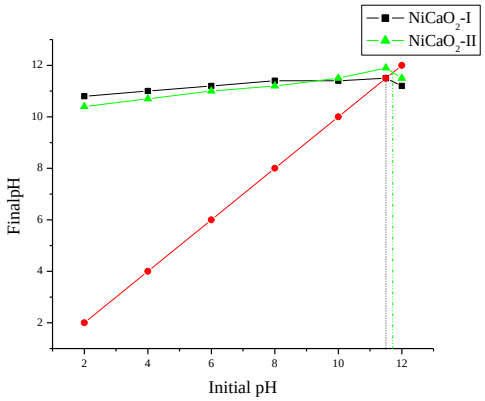

Fig 6: Point of Zero Charge of $NiCaO_2$ nanoparticles

3.4 Mechanism of Photodegradation

$NiCaO_2$ photocatalyst was found to be photo-excited under solar irradiation. When sunlight strikes on the nano-particle surface, an electron from its valance band (vb) jumps to the conduction band (cb) leaving behind positively charged hole (h^+_{vb}). The negative charge is increased in the conduction band (e^-_{cb}) and photocatalytic active centers are formed on the surface of $NiCaO_2$nanoparticles. The valence band holes react with the chemisorbed H_2O molecules to form reactive species such as ·OH radicals, which subsequently react with dye molecules to cause their complete degradation. The e^-_{cb} and h^+_{vb} can be trapped in surface states where they may react with species adsorbed or close to the surface of the particle. The e^-_{cb} can react with an acceptor, such as dissolved O_2, which consequently is transformed into a super oxide radical anion ($O_2^{\bullet-}$) which leads to the formation of additional H_2O. On the other hand, h^+_{vb} could interact with donors, such as $OH^-$and $H_2O^\bullet$, to form $^\bullet$OH radicals. These radicals also attack the CR. Hence, these radicals will attack the dye molecules and degrade them [31].

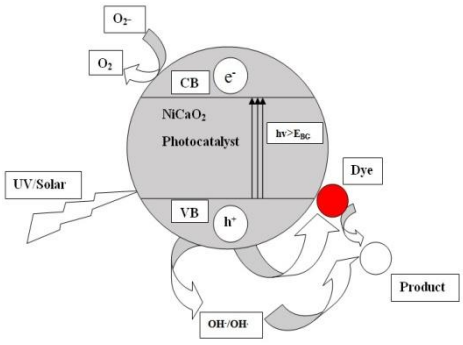

Fig 7: Mechanism of photocatalytic degradation

3.5 Effect of Catalyst Loading

A series of experiment were carried out to assess the optimum catalyst loading by varying the amount of catalyst from 0.1g to 1g/100ml in neutral pH. The percentage of degradation of dye has shown appreciable results. Where, $NiCaO_2$-I (Fig. 8) (Photo 1a) showed maximum of 97.67 % at 0.4g/100ml, $NiCaO_2$-II (Fig. 8) (Photo 1b) showed 97.19% at 0.4g/100ml in 120 minutes. The photodegradation rate of the CR was found to increases with increase in the catalyst loading, then decrease with the increase in the catalyst concentration (Fig. 3), a general characteristic of heterogeneous photocatalyst, and our results are good agreement with the earlier reports

IJARSE
ISSN (O) 2319 - 8354
ISSN (P) 2319 - 8346

in the literature [32-34] further the increase in the catalyst loading the rate of degradation was decreases due to excess loading of catalyst leads to reduced the light penetration through the solution [35] and decrease in the number of active sites on the surface area due to the aggregation of $NiCaO_2$ particle at high concentration, hence it requires a number active surface area [36].While below the level, it assumed that the catalyst surface and adsorption of the light by the catalyst are limiting factor [37,38].

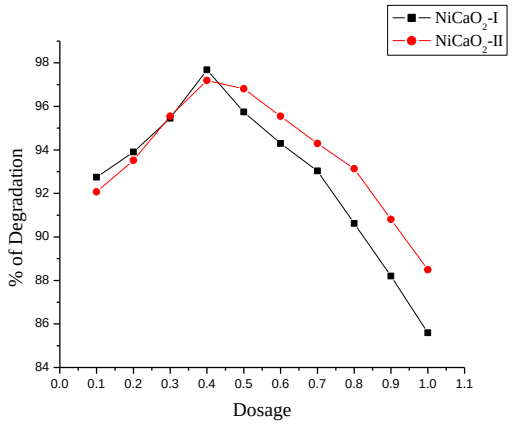

Fig 8: Effect of catalyst concentration on dye solution at 120 minutes=20ppm, pH=7, (a) = $NiCaO_2$-I, (b) = $NiCaO_2$-II.

(a)

(b)

Photo 1: Effect of catalyst concentration on CR dye at 120 minutes=20ppm, pH=7, (a) = $NiCaO_2$-I, (b) = $NiCaO_2$-II.

3.6 Effect of ph

The pH plays a major role in the treatment of waste water and also generation of hydroxyl radicals. The degradation of CR dye was investigated varying pH ranging from 2 to11. The percentage of degradation on CR dye for $NiCaO_2$-I (Fig.9) (Photo 2a) increased from 95.06% to 98.06% from pH 2 to pH 4 and decreased to 86.75% at pH 11 in 120 minutes for 0.4g/100ml. For $NiCaO_2$-II (Fig. 9) (Photo 2b) the degradation of the CR increased from 94.58% to 97.48% from pH 2 to pH 4 and decreased 84.33% at pH 11 in 120 minutes for 0.4g/100ml. The maximum percentage of degradation for the two different nanoparticles was achieved at pH 4. Similar kind of work reported in the previous work [39,40].

The effect of pH in the photodegradation of dye in presence of $NiCaO_2$ can be explained on the basis of zero point charge (pH_{zpc}) of the nanoparticles. The pH_{zpc} of the $NiCaO_2$ nanoparticle was 11.5 and 11.7 (fig 6). Thus, the surface of the catalyst is positively charged below the zpc and negatively charged above the zpc. The interaction of CR dyes on the surface of the catalyst increasing the generation of $OH^{\bullet}$ radicals. These OH^- ions will generate more $^{\bullet}OH$ radicals by combining with the hole of the semiconductor and the $OH^{\bullet}$ radicals are the main oxidizing species responsible for photocatalytic degradation

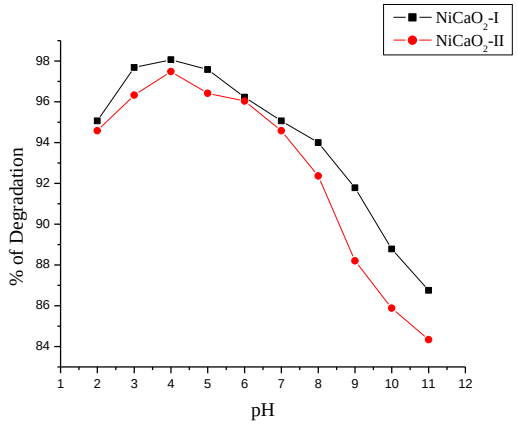

Fig 9: Effect of pH on dye at 120 minutes=20ppm, (a) pH=6 $NiCaO_2$-I, (b) pH=3 $NiCaO_2$-II.

(a)

(b)

Photo 2: Effect of pH on dye at 120 minutes=20ppm, (a) pH=4 $NiCaO_2$-I, (b) pH=4 $NiCaO_2$-II

The experimental data revealed that higher degradation of CR was observed in acidic medium. Since, the photocatalytic activity, below the pzc electrostatic interaction between positive charged surface $NiCaO_2$ and CR anions leads to the strong adsorption and in greater the zpc the reverse effect is observed [41]. After the optimum pH (above pH 5) the degradation efficiency was decreased, can be explained on the basis of amphoteric nature of the catalyst [42].

3.7 Effect of Initial Concentration of Dye

Dye concentration is an very important parameter in treatment of waste water. The effect of initial concentration of dye on the degradation was performed by varying the initial dye concentration from 20ppm to 50ppm with constant catalyst loading and pH (0.4g/100ml/4). The results obtained for $NiCaO_2$-I (Fig. 10) (Photo 3a) was 98.06% for 20ppm, 97.19% for 30ppm, 72.84% for 40ppm and 60.12% for 50ppm. And for $NiCaO_2$-II (Fig. 10)

(Photo 3b) is 97.48% for 20ppm, 96.21% for 30ppm, 86.64% for 40ppm and 72.61% for 50ppm, these experiments illustrated that the degradation efficiency was directly affected by the concentration.

The results, showed that, the percentage of degradation decrease as the dye concentration increases. Similar results have been reported for the photocatalytic oxidation of other dyes [36,43,44]. When the concentration of the dye solution increases, this leads to the amount of dye adsorbed on the catalyst surface increases and affects the photocatalytic activity of the $NiCaO_2$ nanoparticles, this also decreases the path length of photons entering into the dye solution. The degradation is mainly related to the formation of OH radicals, these OH radicals are the main critical species in the degradation process.

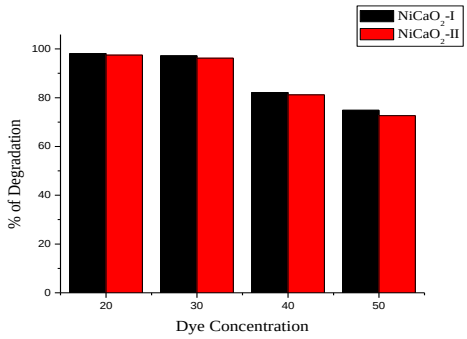

Fig 10: Effect of initial dye concentration on the photocatalytic degradation of CR (a = $NiCaO_2$-I g/pH=0.3/6, b = $NiCaO_2$-II g/pH=0.4/3

Important point for this behaviour is that as the initial concentration of dye increases, the more and more number of dye molecules are adsorbed on the surface of the $NiCaO_2$ nanoparticles are decreases, consequently attacking of OH radicals to the dye molecules are decreased [45] and competence between dye and OH^- ion adsorption on the surface of catalyst [37]. The path length of photons entering the solution decreases, and in low concentration the reverse effect is observed, the number of photon absorption by the surface of catalyst in lower concentration when increase the dye concentration. [43]. Hence, the rate of degradation decreases with increase in the dye concentration.

(a)

(b)

Photo 3: Effect of initial dye concentration on the photocatalytic degradation of CR (a = $NiCaO_2$-I g/pH=0.4/4, b = $NiCaO_2$-II g/pH=0.4/4)

IJARSE
ISSN (O) 2319 - 8354
ISSN (P) 2319 - 8346

3.8 Effect of Different Conditions

The photocatalytic degradation of CR dye (20ppm) under three different experimental conditions were examined, *i.e.*, through, dye/dark/catalyst, dye/UV/catalyst and dye/sunlight/catalyst for the catalyst. CR dye solution when exposed directly to the sunlight without the catalyst, the degradation was found to be nil during the entire experiments. The degradation rate was found to be increase with increase in irradiation time, for dye/sunlight/ $NiCaO_2$-I showed 98.06%, dye/UV/ $NiCaO_2$-I found to be 67.98% and for dye/dark/ $NiCaO_2$-I 44.77% was recorded (Fig. 11) (Photo 4a).Similarly for CR dye (20mg/L) for dye/sunlight/ $NiCaO_2$-II showed 97.48%, dye/UV/ $NiCaO_2$-II found to be 55.89% and for dye/dark/ $NiCaO_2$-II 37.04% was recorded (Fig. 11) (Photo 4b). These results clearly indicate that, photodegradation occurs most efficiently in the presence of sunlight. Under sunlight, excitation of electrons from the catalyst surface takes place more rapidly than in the absence of light. Similar observations have been reported for photocatalytic degradation of dyes [46].

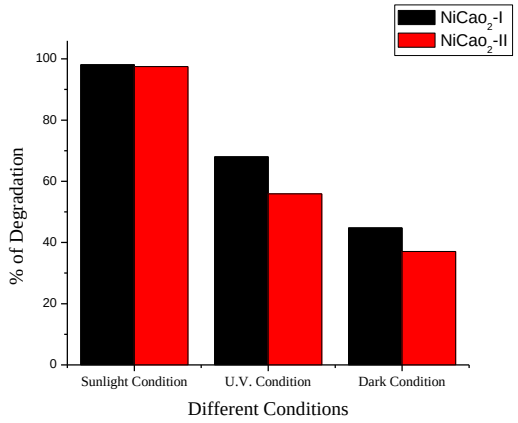

Fig 11: Effect of sunlight irradiation with respect to Dark condition and UV condition on photocatalytic degradation of CR in 120 minutes.

(a)

(b)

Photo 4: Effect of sunlight irradiation with respect to Dark condition and UV condition on photocatalytic degradation of CR in 120 minutes (a = $NiCaO_2$-I g/pH=0.4/4, b = $NiCaO_2$-II g/pH=0.4/4)

IV. CONCLUSION

Photocatalysis is a very effective method for the degradation of industrial or textile dyes. In this study, $NiCaO_2$ nanoparticles were synthesized and characterized by XRD, SEM, EDX, BET and UV-Vis reflectance. It was observed that the synthesized $NiCaO_2$-I (average particle size 14 nm) and $NiCaO_2$-II (average particle size

IJARSE
ISSN (O) 2319 - 8354
ISSN (P) 2319 - 8346

19nm) are photosensitive and effective in degrading selected azo dye (CR) completely in a short interval of time (120 minutes). From this experiment, we can conclude that the $NiCaO_2$ did in fact degrade the dye over short interval of time with the help of sunlight. Even though the result was achieved more than 97%, we still believe that if this experiment was done over a longer period of time that the concentration of the dyes would have been zero. This protocol developed may be employed effectively in the treatment of textile dye effluents which are hazardous to the environment.

V. ACKNOWLEDGEMENT

We are very much thankful to the department of Environmental science, Kuvempu University, Shankaraghatta for providing laboratory facilities.

REFERENCE

[1] B. K. Avasarala, S. R. Tirukkovalluri, and S. Bojja, *Environmental & Analytical Toxicology Magnesium Doped Titania for Photocatalytic Degradation of Dyes in Visible Light, Journal of Environmental & Analytical Toxicology, 6(2),* 2016, doi: 10.4172/2161-0525.1000358.

[2] F. Li, Y. Jiang, M. Xia, M. Sun, B. Xue, and X. Ren, *A high-stability silica-clay composite: Synthesis, characterization and combination with TiO_2 as a novel photocatalyst for Azo dye, Journal of Hazardous Materials. 165(1-3),* 2009, 1219-1223, doi.org/10.1016/j.jhazmat.2008.10.001.

[3] E. Franciscon, M. J. Grossman, J. A. R. Paschoal, and F. G. R. Reyes, *Decolorization and biodegradation of reactive sulfonated azo dyes by a newly isolated Brevibacterium sp. strain VN 15, SpringerPlus*, 2012, 1–10. DOI: 10.1186/2193-1801-1-37.

[4] A. D. Bokare, R. C. Chikate, C. V. Rode, and K. M. Paknikar, *Iron-nickel bimetallic nanoparticles for reductive degradation of azo dye Orange G in aqueous solution, Applied catalysis B: Environmental, 79,* 2008, 270-278. doi 10.1016/j.apcatb.2007.10.033.

[5] Y. Peng, D. Fu, R. Liu, F. Zhang, and X. Liang, *$NaNO_2/FeCl_3$ catalyzed wet oxidation of the azo dye Acid Orange, Chemosphere, 71,* 2008**,** 990–997. doi:org/10.1016/j.chemosphere.2007.10.065

[6] E.M. Saggioro, A.S. Oliveira, T. Pavesi, C.G. Maia, F.L.V. Ferreira, and J.C. Moreira, *Use of Titanium Dioxide Photocatalysis on the Remediation of Model Textile Wastewaters Containing Azo Dyes, Molecules, 16(12),* 2011, 10370–10386. doi:10.3390/molecules161210370.

[7] F. Kiriakidou, D.I. Kondarides, and X.E. Verykios, *The effect of operational parameters and TiO_2 - doping on the photocatalytic degradation of azo-dyes, Catalysis Today, 54,* 1999, 119–130.

[8] Afkhami, and R. Moosavi, *Adsorptive removal of Congo red, a carcinogenic textile dye , from aqueous solutions by maghemite nanoparticles, 174*, 2010, 398–403.

[9] C. Cripps, J.A. Bumpus, S.D. Aust, *Biodegradation of azo and heterocyclic dyes by Phanerochaete chrysosporium, Applied Environmental Microbiology, 56(4),* 1990, 1114-1118.

[10] S. Dafare, P. S. Deshpande, and R. S. Bhavsar, *Photocatalytic degradation of congo red dye on combustion synthesised Fe_2O_3, Indian Journal of Chemical Technology, 20,* 2013, 406–410.

[11] S. Rouf, M. Nagapadma, and R.R. Rao, *Removal of Harmful Textile Dye Congo red from Aqueous Solution Using Chitosan and Chitosan Beads Modified with CTAB, Int. Journal of Engineering Research and Applications, 5(3),* 2015, 75–82.

IJARSE
ISSN (O) 2319 - 8354
ISSN (P) 2319 - 8346

[12] H. Zhu, J. Yao, R. Jiang, Y. Fu, Y. Wu, and G. Zeng, *Enhanced decolorization of azo dye solution by cadmium sul fi de / multi-walled carbon nanotubes / polymer composite in combination with hydrogen peroxide under simulated solar light irradiation, Ceramics International, 40,* 2014, 3769–3777. doi.org/10.1016/j.ceramint.2013.09.043

[13] N. Daneshvar, D. Salari, and A. R. Khataee, *Photocatalytic degradation of azo dye acid red 14 in water : investigation of the effect of operational parameters, Journal of Photochemistry and Photobiology A: Chemistry, 157,* 2003, 111–116. doi.org/10.1016/S1010-6030(03)00015-7.

[14] A. Tadjarodi, M. Imani, H. Kerdari, K. Bijanzad, D. Khaledi, and M. Rad, *Preparation of CdO Rhombus-like Nanostructure and Its Photocatalytic Degradation of Azo Dyes from Aqueous Solution, Nanomaterials and Nanotechnology, 4(16),* 2014, 1-10. DOI: 10.5772/58464

[15] J. O. Carneiro, A. P. Samantilleke, P. Parpot, F. Fernandes, M. Pastor, A. Correia, E. A. Luis, A. A. C. Barros, and V. Teixeira, V*isible Light Induced Enhanced Photocatalytic Degradation of Industrial Effluents (Rhodamine B) in Aqueous Media Using TiO_2 Nanoparticles, Journal of Nanomaterials,* 2016, doi.org/10.1155/2016/4396175.

[16] U. I. Gaya, and A. H. Abdullah, *Heterogeneous Photocatalytic Degradation of Organic Contaminants Over Titanium Dioxide : A Review of Fundamentals, Progress and Problems, Journal of Photochemistry and Photobiology C: Photochemistry Reviews, 9,* 2008, 1-12. doi:10.1016/j.jphotochemrev.2007.12.003.

[17] L. G. Devi, B. N. Murthy, and S. G. Kumar, *Photocatalytic activity of TiO_2 doped with Zn^{2+} and V^{5+} transition metal ions : Influence of crystallite size and dopant electronic configuration on photocatalytic activity, Materials Science and Engineering B, 166,* 2010, 1–6. doi.org/10.1016/j.mseb.2009.09.008.

[18] H. Guo, Y. Ke, D. Wang, K. Lin, R. Shen, J. Chen, and W. weng, *Efficient adsorption and photocatalytic degradation of Congo red onto hydrothermally synthesized NiS nanoparticles, Journal of Nanoparticles Research, 15,* 2013, 1475. doi.org/10.1007/s11051-013-1475-y.

[19] W. Konicki, D. Sibera, E. Mijowska, Z. Lendzion-bielun, and U. Narkiewicz, *Equilibrium and kinetic studies on acid dye Acid Red 88 adsorption by magnetic $ZnFe_2O_4$ spinel ferrite nanoparticles, Journal of Colloid and Interface Science, 398,* 2013, 152–160. doi.org/10.1016/j.jcis.2013.02.021.

[20] H. Lachheb, E. Puzenat, A. Houas, M. Ksibi, E. Elaloui, C. Guillard, and J. Herrmann, *Photocatalytic degradation of various types of dyes (Alizarin S, Crocein Orange G, Methyl Red, Congo Red, Methylene Blue) in water by UV-irradiated titania, Applied Catalysis B: Environmental, 39,* 2002, 75–90.

[21] R.K. Wahi, W.W. Yu, Y. Liu, M.L. Mejia, J.C. Falkner, W. Nolte, and V.L. Colvin, *Photodegradation of Congo Red catalyzed by nanosized TiO_2, Journal of Molecular Catalysis A: Chemical, 242,* 2005, 48–56. doi.org/10.1016/j.molcata.2005.07.034.

[22] Y. Yao, S. Miao, S. Liu, L.P. Ma, H. Sun, and S. Wang, *Synthesis, characterization, and adsorption properties of magnetic Fe_3O_4@ graphene nanocomposite. Chemical Engineering Journal, 184,* 2012, 326–332. doi.org/10.1016/j.cej.2011.12.017.

[23] H. Zhu, R. Jiang, L. Xiao, Y. Chang, Y. Guan, X. Li, and G. Zeng, *Photocatalytic decolourization and degradation of Congo Red on innovative crosslinked chitosan / nano-CdS composite catalyst under*

visible light irradiation, Journal of Hazardous Materials, 169, 2009, 933–940. doi.org/10.1016/j.jhazmat.2009.04.037.

[24] Gurushantha, K., Anantharaju, K. S., Nagabhushana, H., Sharma, S. C., Vidya, Y. S., Shivakumarae, C., Nagaswarupaa, H. P., Prashanthaa, S. C., and Anilkumar, M. R. (2015). Chemical Facile green fabrication of iron-doped cubic ZrO_2 nanoparticles by Phyllanthus acidus : Structural , photocatalytic and photoluminescent properties. *"Journal of Molecular Catalysis. A, Chemical*,397: 36–47. Doi:10.1016/2014.10.025.

[25] C. Parthibana, and N. Sundaramurthy, Biosynthesis , *Characterization of ZnO Nanoparticles by Using Pyrus Pyrifolia Leaf Extract and Their Photocatalytic Activity, International, Journal of Innovative Research in Science, Engineering and Technology, 4(10),* 2015, 9710-9718

[26] Y. Liu, M. Qin, L. Zhang, B. Jia, Z. Cao, D. Zhang, and X. Qu, *Solution combustion synthesis of Ni − Y 2 O 3 nanocomposite powder, Trans. Nonferrous Met. Soc, 25,* 2015, 129–136.

[27] T. Yang, D. Xia, G. Chen, and Y. Chen, *Influence of the surfactant and temperature on the morphology and physico-chemical properties of hydrothermally synthesized composite oxide $BiVO_4$, Materials Chemistry and Physics,114,* 2010, 69–72.

[28] T. K. Ghorai, and N. Biswas, *Photodegradation of rhodamine 6G in aqueous solution via $SrCrO_4$ and TiO_2 nano-sphere mixed oxides, Journal of Materials Science and Technology, 2(1),* 2013, 10-17.

[29] M. Ge, N. Zhu, Y. Zhao, J. Li, and L. Liu, *Sunlight-Assisted Degradation of Dye Pollutants in Ag_3PO_4 Suspension, Industrial and Engineering Chemistry research, 51,* 2012, 5167−5173.

[30] S.D. Kulkarni, S. Kumbar, S.G. Menon, K.S. Choudhari, and C. Santhosh, '*Magnetically separable core–shell $ZnFe_2O_4$@ZnO nanoparticles for visible light photodegradation of methyl orange', Materials Research Bulletin, 77,* 2016, 70–77.

[31] N. Madhusudhana, K. Yogendra, and K.M. Mahadevan, *Photocatalytic decolourization of Textile Effluent by using Synthesized Nano particles, Journal of Environmental. Nanotechnology, 3(4),* 2014, 41-53.

[32] C. C. Chen, C. S. Lu, Y. C. Chung, and J. L. Jan, *UV light induced photodegradation of malachite green on TiO_2 nanoparticles, Journal of Hazardous Materials, 141,* 2007, 520–528. doi.org/10.1016/j.jhazmat.2006.07.011

[33] P. K. Boruah, P. Borthakur,, G. Darabdhara, C. K. Kamaja, I. Karbhal, M. V. Shelke, P. Phukan, D. Saikiad, and M. R. Das, *Advances Sunlight assisted degradation of dye molecules and reduction of toxic Cr (VI) in aqueous medium using magnetically recoverable Fe3O4/ reduced graphene oxide nanocomposite, RSC Advances, 6,* 2016, 11049–11063.

[34] K. Selvam, M. Muruganandham, N. Sobana, and M. Swaminathan, *Enhancement of UV-assisted photo-Fenton degradation of reactive orange 4 using TiO_2 -P25 nanoparticles, Separation and Purification Technology, 54,* 2007, 241–247.

[35] F. Buazar, S. Alipouryan, F. Kroushawi, and S.A. Hossieni, *Photodegradation of odorous 2-mercaptobenzoxazole through zinc oxide / hydroxyapatite nanocomposite, Applied nanoscience*, 2014, doi.org/10.1007/s13204-014-0368-4.

[36] A. Habib, T. Shahadat, N. M. Bahadur, I. M. I. Ismail, and A. J. *Mahmood, Synthesis and characterization of ZnO-TiO_2 nanocomposites and their application as photocatalysts, International Nano Letters, 3(5),* 2013a, 1–8. doi:10.1186/2228-5326-3-5.

[37] H. Wang, C. Xie, W. Zhang, S. Cai, Z. Yang, and Y. Gui, *Comparison of dye degradation efficiency using ZnO powders with various size scales, Journal of Hazardous Materials, 141,* 2007, 645–652. https://doi.org/10.1016/j.jhazmat.2006.07.021.

[38] A. Akyol, H. C.Yatmaz, and M. Bayramoglu, *Photocatalytic decolourization of Remazol Red RR in aqueous ZnO suspensions, Applied Catalysis B: Environmental, 54,* 2004, 19–24.

[39] R.M. Mohamed, I. A. Mkhalid, E.S. Baeissa, and A. Al-Rayyani, *Photocatalytic Degradation of Methylene Blue by Fe/ZnO/SiO_2 Nanoparticles under Visible light, Journal of Nanotechnology, 1-5,* 2012, doi:10.1155/2012/329082.

[40] M. M. Kamel, H. M. Mashaly, and F. Abdelghaffar, *Photocatalyst Decolorization of Reactive Orange 5 Dye Using MgO Nano Powder and H_{2O2} Solution, World Applied Sciences Journal, 26(8), 2*013, 1053–1060. DOI: 10.5829/idosi.wasj.2013.26.08.13546.

[41] A. Habib, M. Muslim, M. T. Shahadat, M. N. Islam, I. Mohmmad, I. M. I. Ismail, T. S. A. Islam, and A. J. Mahmood , *Photocatalytic decolourization of crystal violet in aqueous nano-ZnO suspension under visible light irradiation, International Nano Letters, 3(5),* 2013b, 1-8.

[42] S. Sakthivel, B. Neppolian, M.V, Shankar, B. Arabindoo, M. Palanichamy, and V. Murugesan, *Solar photocatalytic degradation of azo dye : comparison of photocatalytic efficiency of ZnO and TiO_2, Solar Energy Materials & Solar Cells, 77,* 2003, 65–82.

[43] K. Natarajan, T.S. Natarajan, H.C. Bajaj, and R. J. Tayade, Photocatalytic reactor based on UV-LED / TiO_2 coated quartz tube for degradation of dyes, *Chemical Engineering Journal*, 178, 2011, 40–49. doi:10.1016/j.cej.2011.10.007.

[44] B. Neppolian, H. C. Choi, S. Sakthivel, B. Arabindoo, and V. Murugesan, *Solar light induced and TiO_2 assisted degradation of textile dye reactive blue, Chemosphere, 4,* 2002, 1173–1181.

[45] A.P. Toor, A. Verma, C.K. Jotshi, P.K. Bajpai, and V. Singh, *Photocatalytic degradation of Direct Yellow 12 dye using UV / TiO_2 in a shallow pond slurry reactor, Dyes and Pigments, 68,* 2006, 53-60. https://doi.org/10.1016/j.dyepig.2004.12.009.

[46] N. Madhusudhana, K. Yogendra, and K.M. Mahadevan, P*hotocatalytic decolourization of textile effluent by using metal oxide nanoparticles, Journal of Science and Arts, 3(24),* 2013, 303-318.